Water Sorption from Air by Celite-Supported $CaCl_2$: Mathematical Model/Experimental Studies

A feasible means for the long-term storage of thermal energy considers the hydration of $CaCl_2$. Differential and integral beds of Celite pellets impregnated with $CaCl_2$ were employed to dehydrate humid air. Experimental studies were used in modeling the behavior of this system, which involved the solution of four partial differential equations. The simultaneous solution of these equations, using a modified Gear's method, yielded information about the temperature and composition distribution of both the air stream and the impregnated pellets. The mathematical solution predicts the time-dependent moving front characterized by a maximum temperature. Predicted and experimental measurements were found to be in good agreement.

R. V. Heiti and George Thodos
Northwestern University
Evanston, IL 60201

SCOPE

A novel approach for the storage of thermal energy is presented whereby a hygroscopic salt, such as $CaCl_2$, is deposited within a porous structure. This combination enables the convenient sorption of water vapor from a flowing air stream without the formation of an impermeable solid layer at the reaction front. A bed of pellets of a porous material such as that used in this study (Celite), provides a means for enhancing mass and heat transfer associated with the sorption of water vapor from a flowing air stream.

The mathematical characterization of this mode of chemical energy storage has been expressed to define the temperature and water content profiles for the entire system. To accomplish this objective for any hygroscopic salt under consideration as a potential candidate for energy storage, it is necessary to obtain experimental information on the rate of sorption and data on the heat of reaction.

CONCLUSIONS AND SIGNIFICANCE

This study indicates that the transport of water from humid air proceeds with a diffusion-controlling mechanism through the pores of the matrix of the solid support. Experimental evidence bears out this mass transport and indicates that the initial mechanism, which is gas-film controlling, becomes rapidly dominated by diffusion through the solid. This transport proceeds without the difficulties of caking, which have been shown to be limiting in an unsupported $CaCl_2$ hydration system.

The representation of the unsteady state bed behavior is expressed analytically as a moving temperature wave front, which applies to both the gas and solid phases of the system. Calculated overall material and energy balances were found to be consistent with experimental measurements and give credence to the objectives set forth for this mode of energy storage. More specifically, this method of storing thermal en-

Correspondence concerning this paper should be addressed to George Thodos.

ergy finds utility in the long-term storage of solar energy. Energy densities of 226,000 kcal/m^3 (946,940 kJ/m^3) of packed bed are associated with a salt loading of 0.265 g $CaCl_2$/g Celite under the constraint that the sorption of water continues to an ultimate average molar ratio of 14 gmol H_2O/gmol $CaCl_2$. Under these conditions the resulting solution is entrained within the pores of the pellets with no dripping. This energy density is equivalent to the energy stored in 4.91 m^3 of liquid water raised from 20 to 66°C.

Introduction

Chemical energy storage is currently receiving considerable attention because this scheme of storage is not associated with sustained temperature gradients. Conventional means of storing energy, including both sensible and latent heat methods, do not prove to be satisfactory because such approaches involve the continuous presence of such temperature gradients.

The elimination of temperature gradients and heat losses associated with them suggests utilization of a chemical reaction whereby chemical energy can be converted to thermal energy upon demand. Consequently, chemical potential energy becomes attractive, particularly when considering the utilization of intermittent sources of energy such as solar or waste heat. Such an approach makes this method of energy storage time-independent, since no continuous energy losses are involved with this kind of static chemical system.

Several approaches to the solution of this problem have been suggested in the literature. Reversible reactions have been proposed for the conversion of heat into chemical energy in large-scale, high-temperature solar facilities. An example of this is suggested by Chubb (1975), who proposes the catalyzed conversion of SO_3 to SO_2 and oxygen through the absorption of heat at 800–1,000°C and the catalyzed recombination of these products at 500–600°C with the release of heat. A reaction involving lower temperature levels is given by the endothermic decomposition of $Mg(OH)_2$ to MgO and water using superheated steam (Ervin, 1977) and the subsequent exothermic hydration reaction occurring in the presence of saturated steam. Additional suggested reactions involving the decomposition of carbonates to the corresponding oxide and CO_2 have been proposed as a means of chemical storage. More specifically, Wentworth and Chen (1976) have investigated the endothermic decomposition of $MgCO_3$ into MgO and CO_2. When these products are combined, heat is released. In this context, the amine complexes of a number of alkaline earth halides are good candidates for energy storage. Martin-Marietta has proposed the reactions involving the cycling of ammonia between amine complexes of $MgCl_2$ and $CaCl_2$ contained in separate vessels (Hall et al., 1976). All these energy storage schemes have limitations. Such factors as their reactivity at the temperatures attainable in solar collectors, toxicity, safety hazards, and corrosiveness are to be reckoned with, which make the proposed approaches of limited value for domestic heating.

The direct involvement of reactants frequently presents a number of physical problems relating to their combination. For example, the gas-solid reaction involving the combination of water vapor and a hygroscopic salt such as $CaCl_2$ results in the formation of a hydrated front that acts as a barrier to any further reaction within the particle. This phenomenon was observed when attempting to react solid $CaCl_2$ particles by contacting them with water vapor generated from a pool of water existing at its vapor pressure. To overcome this obstacle to mass transfer, means must be devised to eliminate the formation of such hydrated-solid barriers, which act as deterrents to the transport of the gaseous reactant.

Celite Impregnated with Solid Reactant

Since the direct utilization of $CaCl_2$ does not lend itself conveniently to the preparation of a fixed bed, means have been sought to overcome the caking problems and the formation of fronts impeding mass transport. These physical limitations were overcome by impregnating a celite carrier with solid $CaCl_2$. These Celite carrier pellets, a Johns-Manville product identified as Celite catalyst carrier Type VIII, were manufactured by calcining diatomaceous earth. The pellets were cylindrical, 0.39 cm dia. and 0.50 cm long. The impregnation of these Celite carriers was accomplished by soaking dry particles in a concentrated solution of $CaCl_2$ and then passing hot dry air at 140°C through them until the anhydrous form of this salt was established.

Experimental

Compressed air was saturated with water vapor before passing it through a fixed bed of $CaCl_2$-laden Celite particles. Before saturating, the air was filtered, regulated down in pressure, and its flow rate was monitored through a rotameter. Water saturation of the air was carried out in a constant-temperature water bath to control the humidity. The degree of water saturation was always monitored by passing the moist air stream through a bed of Drierite ($CaSO_4$) and weighing it before the initiation and after the completion of an experimental run.

The reactor facility consisted of a vertical cylindrical glass tube 1.70 cm ID, 9.0 cm long, provided with glass wool packing at both ends to distribute the flow evenly and to properly contain the pellets. The humid air was made to flow upward through the bed. For bed lengths of less than 9.0 cm, glass beads were inserted between the Celite pellets and the glass wool. This reactor facility was exposed directly to the surroundings and was periodically removed for the determination of water sorption by weighing. In addition, experimental runs were conducted in a calorimeter consisting of a water-filled Dewar flask in which the temperature rise was measured with a Beckmann thermometer. The humidity of the outlet stream was periodically monitored by following the procedure outlined for the determination of the humidity of the inlet stream, using the Drierite water sorption method already described.

This dual arrangement provided means for establishing either the rate of water sorption or the release of thermal energy upon reaction. Three different bed heights (lengths), 1.5, 4.0, and 9.0 cm, were used. Because of these bed lengths, the information relating to water sorption represents an integrated value and approximates a differential bed behavior only for the 1.5 cm bed.

Altogether nine runs were conducted using the 1.5 cm bed.

Table 1. Conditions Associated with Runs of 1.5 cm Bed Height

Run	Air Flow cm^3/min	Inlet Humidity g H_2O/ g dry air	Duration s	Extent of Saturation gmol H_2O/ gmol $CaCl_2$
1	4,200	0.0161	3,500	13.63
2	2,900	0.0162	3,500	11.97
3	1,620	0.0168	5,000	12.15
4	4,200	0.0100	4,300	9.00
5	2,900	0.0104	4,000	8.06
6	1,620	0.0106	5,000	7.68
7	4,330	0.0078	2,800	5.65
8	2,980	0.0056	4,400	4.66
9	1,620	0.0056	4,400	3.86

Loading: 0.204 g $CaCl_2$/g Celite
Air flow given at STP conditions [0°C; 1 atm (101.3 kPa)]

For these runs, the air flow rate and inlet humidity were varied; however, the $CaCl_2$ loading was kept constant. Table 1 presents the conditions associated with these nine runs. Further details relating to the complete behavior of a single run (run 6) are presented in Table 2. For the remaining eight runs, information similar to that given for run 6 is presented elsewhere (Heiti, 1985). The average rates of water sorption vs. molar ratio of water sorbed to $CaCl_2$ are presented in Figure 1. This figure also includes the behavior of runs 3 and 9 for which the air flow is the same (1,620 cm^3/min), and indicates the influence of inlet humidity on the rate of water sorption.

Mathematical Description of System

The changes occurring in concentration within a fluid stream and a bed of sorbent particles becomes a formidable mathematical undertaking. This problem becomes even more complex if the sorption step is associated with the release of heat, which exerts an influence on the time-dependent temperature distribution throughout the bed. A comprehensive treatment of this problem requires that a material balance satisfy the transfer of mass from the fluid to the solid phase and the simultaneous energy transfer between these two phases. This approach gives rise to one partial differential equation dealing with the transport of mass and two additional partial differential equations associated with the transfer of energy between the two phases. These three partial differential equations must then be solved simultaneously in order to completely characterize the concentration of the transferable component and the temperature within the fluid and solid phases. The development of this system of partial differential equations, where sorption takes place from a dilute solution, has been presented by Hougen and Marshall (1947), and may be summarized as follows:

$$\frac{\partial y}{\partial \tau} = -\frac{G}{\epsilon \rho_g}\left(\frac{\partial y}{\partial z}\right) - \frac{\rho_b}{\epsilon \rho_g}\left(\frac{\partial w}{\partial \tau}\right) \tag{1}$$

$$\frac{\partial t_g}{\partial \tau} = -\frac{G}{\epsilon \rho_g}\left(\frac{\partial t_g}{\partial z}\right) + \frac{h_g a_v}{\epsilon \rho_g c_g}(t_s - t_g) \tag{2}$$

$$\frac{\partial t_s}{\partial \tau} = -\frac{h_g a_v}{c_s \rho_b}(t_s - t_g) + \frac{\Delta H}{c_s M_w}\left(\frac{\partial w}{\partial \tau}\right) \tag{3}$$

The solution of these three partial differential equations requires that the rate of sorption, $\partial w/\partial \tau$, be specified. Film theory can be applied to represent the rate of sorption; however, additional information relating to diffusion within the solid particle must be available to properly establish $\partial w/\partial \tau$, the rate of mass transport from the fluid into the solid phase. The prediction of this information becomes highly speculative and therefore experimental measurements are essential to properly assess the nature of this controlling step.

The information depicted in Figure 1 shows that the rate of sorption of water plotted on a logarithmic scale is linearly dependent on x, the molar ratio of sorbed water to moles of $CaCl_2$. Film theory considerations, where no diffusional effects through the solid exist, predict an initial rate much higher than the corresponding linearly extrapolated value resulting from experimental measurements. For example, for run 6, experimental measurements predict an initial rate of 9.54×10^{-5} g H_2O sorbed/s · g Celite), whereas film theory considerations predict a corresponding value of 9.02×10^{-4}.

Unless a priori experimental information is available for the

Table 2. Water Sorption–Time Data for Run 6

Time, s	Water Sorbed, g	gmol H_2O/ gmol $CaCl_2$	Avg Sorption Rate g H_2O/s · g Celite
0	0	0	—
100	0.0242	0.340	1.130×10^{-4}
200	0.0439	0.617	0.920
400	0.0778	1.094	0.794
600	0.1103	1.551	0.761
800	0.1407	1.979	0.710
1,000	0.1705	2.398	0.696
1,500	0.2362	3.322	0.612
2,000	0.2960	4.163	0.560
2,500	0.3481	4.896	0.486
3,000	0.3965	5.577	0.453
3,500	0.4391	6.176	0.397
4,000	0.4782	6.726	0.364
4,500	0.5143	7.233	0.336
5,000	0.5463	7.684	0.299

Sample: $CaCl_2$ = 0.4381g Celite = 2.1421 g
Air flow = 1,620 cm^3/min
Inlet humidity = 0.0106 g H_2O/g dry air

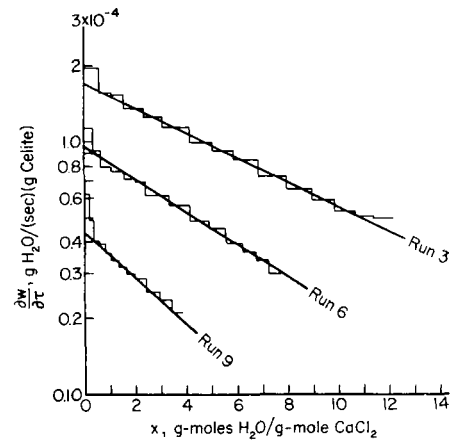

Figure 1. Rate of water sorption vs. $H_2O/CaCl_2$ molar ratio for typical runs; bed height 1.5 cm.

rate of sorption of water as a function of the amount of water sorbed, the global behavior of this system cannot be established. In addition, since nonequilibrium conditions exist on the surface of each pellet, the application of equilibrium relationships for the vapor pressure of water above a hygroscopic salt is equally speculative. Therefore, the combinational contributions of liquid water diffusion within the interstices of the pellet and the nonequilibrium state of water vapor existing at the surface of each pellet, necessitate a direct measurement for the rate of water sorption so that the internal mechanics of this model are properly accounted for. The information obtained in this manner can then be applied for the prediction of any set of operating conditions provided the nature of the controlling parameters for mass and heat transfer coefficients remain the same. More specifically, the effect of particle size is expected to have a direct influence on the rate of sorption of water and the rate of heat exchange between the solid and the fluid flowing past it. This investigation has been centered on the mass and heat transfer behavior of a bed consisting of $CaCl_2$-laden Celite pellets of 0.39 cm OD and 0.50 cm long.

Experimental measurements indicate that the rate behavior is initiated at a value predicted from gas film theory and rapidly converges with the linear relationship depicted in Figure 1. This initial rapidly decreasing rate is demonstrated for runs 8 and 9, shown in Figure 2. Where the rate of sorption ceases to be influenced by gas film theory and becomes completely diffusionally controlled is speculative and must be determined experimentally. However, the linear portion of the rate curve, as shown in Figure 1, can be expressed as follows:

$$\left(\frac{\partial w}{\partial \tau}\right)_d = ae^{-bx} \tag{4}$$

for which it has been found that the intercept $a = 0.5685y^{1.235}G^{0.737}$ and $b \approx 0.0213G^{0.188}/y^{0.60}$, where y is the humidity of the flowing air (g-H_2O/g dry air) and G is the superficial mass velocity of the air, g/s · cm^2.

To account for the highly decaying initial rate predicted by gas-film transport, the additional rapidly decreasing expression (Heiti, 1985)

$$\left(\frac{\partial w}{\partial \tau}\right)_g = \left[\frac{k_g a_v M_g \pi y}{\rho_b} - a\right](1 - x)^{20} \tag{5}$$

is added to Eq. 4 for molar ratios, $x \leq 1.0$. For $x = 0$, the sum of Eqs. 4 and 5 produces a rate that is completely gas-film controlled. At the arbitrarily chosen value of $x = 1$, the rate of water sorption becomes completely controlled by diffusion through the solid as described by Eq. 4, with the gas film contribution to the rate of water sorption becoming no longer significant.

In order to facilitate the numerical solution of this system of equations, it proves expeditious to cast them in dimensionless form with time and position as the independent variables. All the variables were rendered dimensionless through the following transformations:

$$\omega = \frac{w}{w_d} \quad Y = \frac{y}{y_o} \quad \theta_g = \frac{t_g}{t_o} \quad \theta_s = \frac{t_s}{t_o} \quad T = \frac{\tau}{\tau_o} \quad \text{and} \quad Z = \frac{z}{z_l}$$

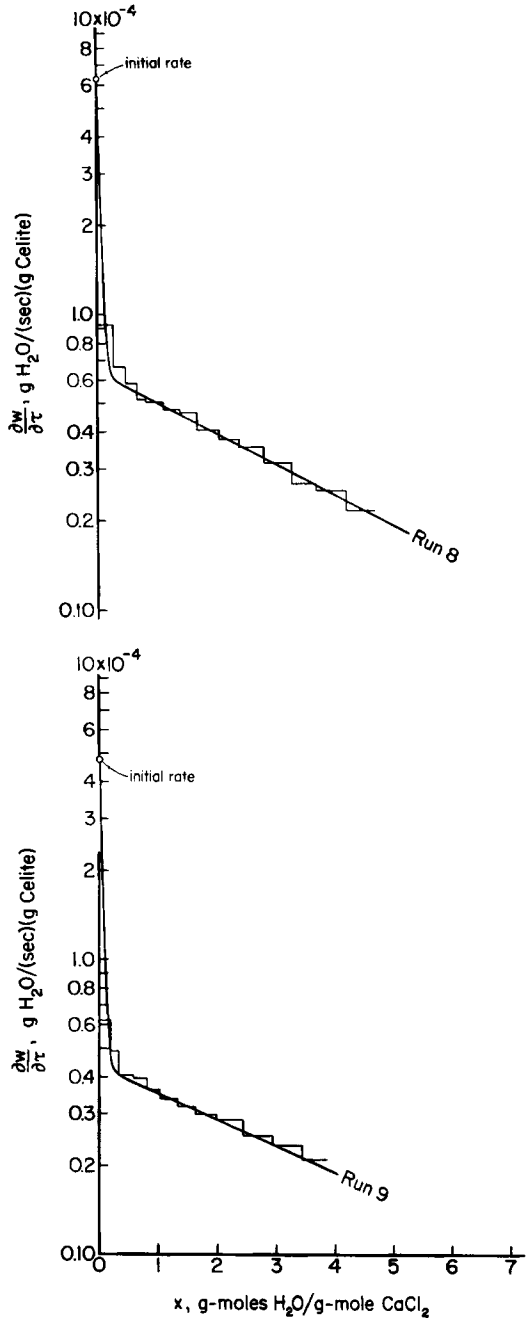

Figure 2. Rate of water sorption vs. $H_2O/CaCl_2$ molar ratio for runs 8 and 9, showing rapid decrease in initial rate.

Equations 1–4 can be rewritten in dimensionless form as follows:

$$\frac{\partial Y}{\partial T} = -\left(\frac{\partial Y}{\partial Z}\right) - \frac{\rho_b \rho_w}{\rho_p \rho_g y_o} \frac{\epsilon}{\epsilon_i}\left(\frac{\partial \omega}{\partial T}\right) \tag{6}$$

$$\frac{\partial \theta_g}{\partial T} = -\left(\frac{\partial \theta_g}{\partial Z}\right) - \frac{h_g a_v z_l}{c_g G}(\theta_s - \theta_g) \tag{7}$$

$$\frac{\partial \theta_s}{\partial T} = -\frac{h_g a_v z_l \epsilon \rho_g}{G c_s \rho_b}(\theta_s - \theta_g) + \frac{\rho_w \epsilon_i}{M_w c_s \rho_p t_o} \Delta H \left(\frac{\partial \omega}{\partial T}\right) \tag{8}$$

and

$$\frac{\partial \omega}{\partial T} = \frac{z_1 \rho_g \rho_p \epsilon}{\rho_w G \epsilon_i} a e^{-b\alpha\omega} \tag{9}$$

where

$$\alpha = \epsilon_i \rho_w M_{CaCl_2} / \rho_p L M_w$$

The nonlinear form of Eq. 9 influences the behavior of Eqs. 6, 7, and 8. This system of equations exhibits stiff behavior and solution requires a treatment consistent with their particular nature. Of the several possible numerical approaches for solution of this system of equations, a modified Gear's method was selected (Ames, 1977).

This system of four first-order partial differential equations in the two independent variables, distance Z and time T, were transformed into a system of first-order ordinary differential equations by discretizing Z, the distance variable. For example, the computer models used in this study involved a 9 cm bed that was divided into 1 cm lengths. This approach gave rise to ten nodal points, each point being represented by the four equations. This system of 40 differential equations was solved using an IMSL subroutine for Gear's method entitled DGEAR. The details associated with the development and solution of this model are presented by Heiti (1985).

Physical Properties of the System

The bed properties were determined and found to be as follows:

Densities	Void Fractions
$\rho_b = 0.549$ g/cm^3	$\epsilon = 0.365$
$\rho_p = 0.866$ g/cm^3	$\epsilon_i = 0.575$

The external surface area available to mass and heat transfer is $a_v = 7.355$ cm^2/cm^3. This value was calculated for cylinders of 0.39 cm dia., 0.50 cm long, and void fraction, $\epsilon = 0.365$. The heat capacity of the solid was taken to be $c_s = 0.21$ cal/g · °C (0.88 J/g · °C) while that of the flowing air was $c_g = 0.249$ cal/g · °C (1.043 J/g · °C). The loading used in the computer simulation was experimentally set at $L = 0.2045$ g $CaCl_2$/g Celite.

Heat and mass transfer coefficients were calculated from the j-factor correlation of Sen Gupta and Thodos (1962),

$$\epsilon j = 0.01 + \frac{0.863}{Re^{0.58} - 0.483} \tag{10}$$

Heats of hydration per gmol of water reacted were obtained from the literature and can be summarized as follows (Bailar et al. 1973):

$$CaCl_2(s) + H_2O(g) \longrightarrow CaCl_2 \cdot H_2O(s) \qquad \Delta H = -17{,}300 \text{ cal}$$

$$CaCl_2 \cdot H_2O(s) + H_2O(g) \longrightarrow CaCl_2 \cdot 2H_2O(s) \qquad \Delta H = -12{,}600 \text{ cal}$$

$$CaCl_2 \cdot 2H_2O(s) + 2H_2O(g) \longrightarrow CaCl_2 \cdot 4H_2O(s) \qquad \Delta H = -14{,}550 \text{ cal}$$

$$CaCl_2 \cdot 4H_2O(s) + 2H_2O(g) \longrightarrow CaCl_2 \cdot 6H_2O(s) \qquad \Delta H = -13{,}700 \text{ cal}$$

The addition of water vapor to $CaCl_2 \cdot 6H_2O(s)$ was determined experimentally for bulk compositions up to 14 gmol H_2O/gmol $CaCl_2$ to be, $\Delta H = -11{,}770$ cal/gmol ($-49{,}316$ J/gmol) of water vapor added.

Numerical Solution of Unsteady State Bed Behavior

To obtain basic information relating to this study through the numerical solution of Eqs. 6–9, the experimental runs associated with 1.5 cm bed lengths were employed since these runs best approximate differential bed conditions. The results of the runs for the 4.0 and 9.0 cm bed lengths were reserved for testing the model once the experimental data for the 1.5 cm bed length were properly modeled.

To test the model prediction, a plot predicting values of x, gmol H_2O/gmol $CaCl_2$ was related to time and compared with corresponding experimental measurements for all bed lengths investigated (1.5, 4.0, and 9.0 cm). For the 1.5 cm bed, the correlation for the constant $a = 0.5685y^{1.235}\, G^{0.737}$, which applies to any bed length, produced integrated values that were consistently below the experimental values. This condition forced a reassessment of this generalized coefficient so that the predicted values coincided with the experimental measurements for all bed lengths. This matching was realized when $a = 1.5(0.5685y^{1.235}\, G^{0.737}) = 0.8528y^{1.235}\, G^{0.737}$. The significance of the multiplicative factor 1.5 is due to the fact that the humidity throughout the 1.5 cm bed used to develop the generalized parameter a varies and thus accounts for the integral nature of this bed. Thus, the time-integrated value for the humidity y at a nodal point results in a rate that is consistent with the position and time-integrated value represented by the

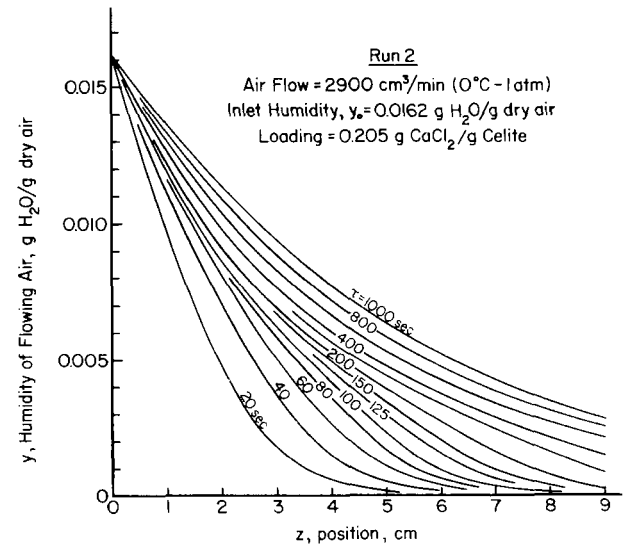

Figure 3. Humidity profiles of flowing air calculated for run 2 conditions.

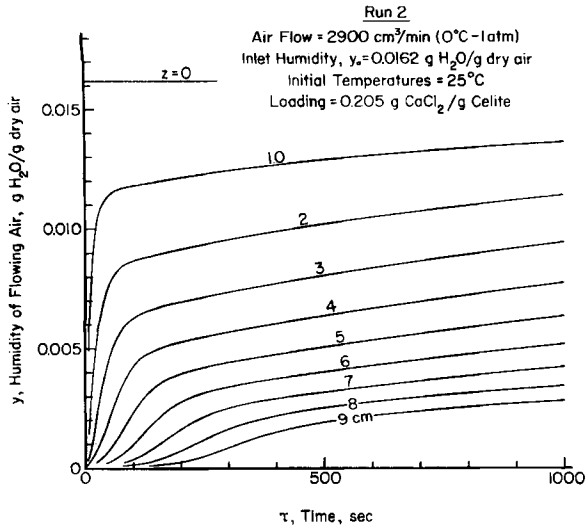

Figure 4. Calculated air humidity vs. time for various bed lengths, run 2.

data for any bed length, as

$$\left(\frac{\partial w}{\partial \tau}\right)_d = 0.8528 y^{1.235} G^{0.737} e^{-bx} \qquad (11)$$

where the constant of the exponent remains unchanged as $b = 0.0213\, G^{0.188}/y^{0.60}$. The utilization of Eq. 11, when incorporated into the numerical solution, produces results consistent with the experimental measurements associated with the 1.5, 4.0, and 9.0 cm bed lengths. Because of this matching, the rate expression given by Eq. 11 becomes applicable in general to a bed of any length, inlet humidity condition, air flow rate, and $CaCl_2$ loading (Heiti, 1985). Therefore, the numerical solution

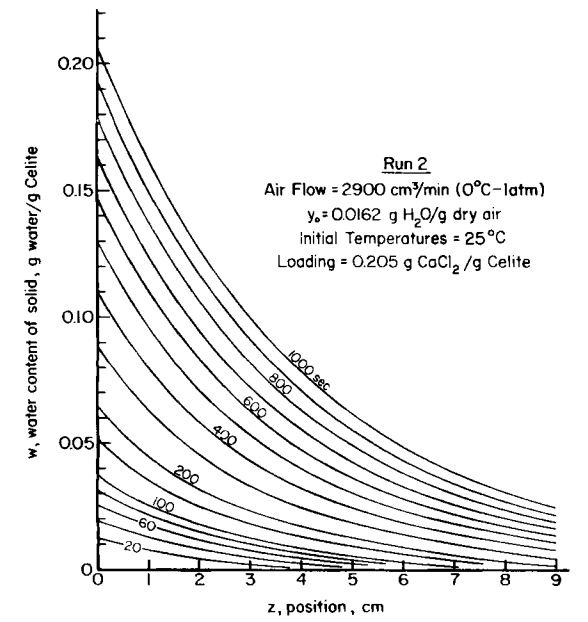

Figure 5. Water content of solid vs. position for various periods of time, run 2.

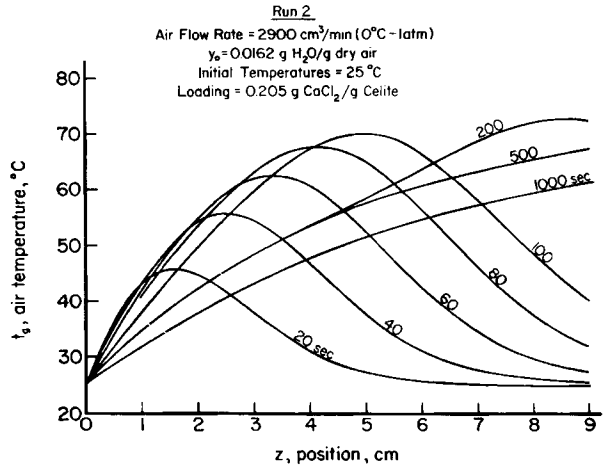

Figure 6. Calculated moving wave front profiles of air temperature vs. position in a bed of $CaCl_2$-impregnated Celite particles, run 2.

involving Equations 6, 7, 8, and 11 produces temperature values t_g and t_s and water contents y and w for the gas and solid phases, respectively, at the nodal points for which the system of equations was specified. Figure 3 presents a set of calculated constant time relationships between y, the humidity of the air within the bed, and position, z. A cross plot of this information, presented in Figure 4, shows the humidity as a function of time for bed lengths up to 9.0 cm. The corresponding relationship for the water content of the solid, w, vs. position, z, is shown in Figure 5. Figures 6 and 7 respectively present the calculated moving wave front profiles of the air temperature, t_g, and the solid temperature, t_s, vs. position, z. The transition between the two controlling modes of transport manifests itself in the irregular pattern exhibited by the 200 s profile of both figures. It should be noted that the temperature profiles of Figures 6 and 7 are similar but shifted with respect to the temperature maximum, and are both presented for the sake of completeness. In addition, Figures 3, 5, 6, and 7 can be utilized to obtain the exit conditions

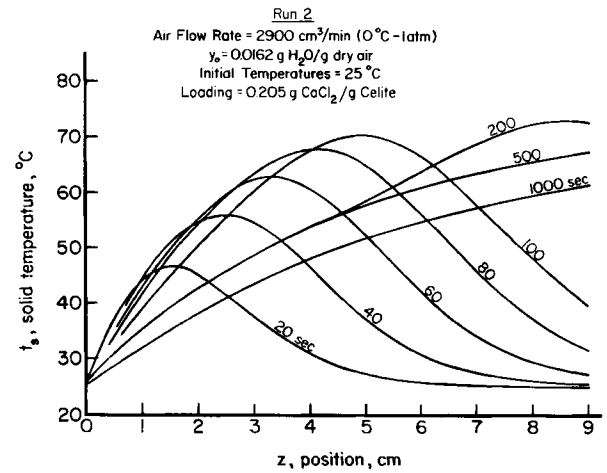

Figure 7. Calculated moving wave front profiles for solid temperature vs. position in a bed of $CaCl_2$-impregnated Celite particles, run 2.

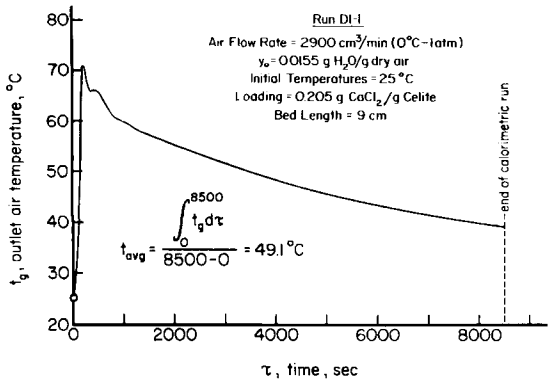

Figure 8. Time-dependent air temperature leaving 9.0 cm bed, run D1-1.

for a bed of any length, such as that presented in Figure 4, by appropriate cross plotting.

As a final check on the simulation of bed behavior, the calorimetric information (Heiti, 1985) associated with the 9 cm bed is compared with the calculated energy delivery to the flowing air stream corresponding to the duration of the calorimetric run (run D1-1) of 8,500 s. This is performed by constructing a cross plot of the exiting air temperature, t_g, from Figure 6, corresponding to the 9.0 cm position as shown in Figure 8. Integration of the curve of Figure 8 yields the average temperature of the air leaving over the time span of interest (τ = 8,500 s). This information, in conjunction with the air flow rate, inlet temperature, and the sensible heat remaining within the solid results in an enthalpy increase of 3,222 calories (13,500 J) due to the exothermic heat of reaction. This value is to be compared with the measured value of 2,861 calories (11,988 J). This disparity corresponds to a deviation of 12.6% and is representative of the average overall deviation resulting from similar comparisons where the loading was varied from 0.205 to 0.456 g $CaCl_2$/g Celite (Heiti, 1985).

Notation

a = constant, Eq. 4
a_v = external area of Celite pellets, cm^2/cm^3
b = constant, Eq. 4
c_g = heat capacity of flowing gas, cal/g · °C
c_s = heat capacity of Celite pellets, cal/g · °C
G = superficial mass velocity, g/s · cm^2
(g) = gas
ΔH = heat of reaction, cal/gmol H_2O
h_g = heat transfer coefficient, cal/s · °C · cm^2
k_g = mass transfer coefficient, gmol H_2O/s · atm · cm^2
L = loading, g $CaCl_2$/g Celite
M_g = molecular weight of air
M_w = molecular weight of water
(s) = solid
t_g = temperature of flowing gas, °C
t_o = initial air and solid temperature, °C
t_s = temperature of Celite pellets, °C
T = dimensionless time, τ/τ_o
w = water content of solid, g H_2O/g Celite
w_d = maximum water content of solid, $\epsilon_i\rho_w/\rho_p$, g H_2O/g Celite
x = molar ratio, gmol H_2O sorbed/gmol $CaCl_2$
y = humidity, g H_2O/g dry air
y_o = inlet air humidity, g H_2O/g dry air
Y = dimensionless humidity, y/y_o
z = downstream distance, cm
z_ℓ = bed length, cm
Z = dimensionless bed position, z/z_ℓ

Greek letters

α = constant, Eq. 9
ϵ = external void fraction
ϵ_i = internal void fraction
θ_g = dimensionless gas temperature, t_g/t_o
θ_s = dimensionless solid temperature, t_s/t_o
π = total pressure, atm
ρ_b = bulk density of packing, g/cm^3
ρ_g = density of flowing gas, g/cm^3
ρ_p = density of pellet, g/cm^3
ρ_w = density of water, g/cm^3
τ = time, s
τ_o = reference time, $z_\ell/(G/\epsilon\rho_g)$, s
ω = dimensionless water content of solid, w/w_d

Subscripts

d = diffusion-through-solid controlling
g = gas-film controlling

Literature Cited

Ames, W. F., *Numerical Methods for Partial Differential Equations*, 2nd ed., Academic Press, New York (1977).

Bailar, Jr., J. C., et al., *Comprehensive Inorganic Chemistry*, 1st ed., Pergamon Press, New York, I (1973).

Chubb, T. A., "Analysis of Gas Dissociation Solar Thermal Power System," *Solar Energy*, **17**, 129 (1975).

Ervin, G., "Solar Heat Storage Using Chemical Reactions," *J. Solid State Chem.*, **22**, 51 (1977).

Hall, C. A., M. T. Howerton, and S. Podlaseck, *Sharing the Sun Conf.*, Winnipeg, Canada, **8**, 176 (Aug., 1976).

Heiti, R. V., "Long-Term Storage of Thermal Energy Through the Involvement of the $CaCl_2$-Hydration Reaction," Ph.D. diss. Northwestern Univ., Evanston, IL (1985).

Hougen, O. A., and W. R. Marshall, "Adsorption from a Fluid Stream Flowing Through a Stationary Granular Bed," *Chem. Eng. Prog.*, **43**, 197 (1947).

Sen Gupta, A., and G. Thodos, "Mass and Heat Transfer in the Flow of Fluids Through Fixed and Fluidized Beds of Spherical Particles," *AIChE J.*, **8**, 608 (1962).

Wentworth, W. E., and E. Chen, "Simple Thermal Decomposition Reactions for Storage of Solar Thermal Energy," *Solar Energy*, **18**, 205 (1976).

Manuscript received Jan. 10, 1985, and revision received May 20, 1985.